

# Visualization of Grain Boundaries on Stainless Steel Plate Surface by Nanosecond Laser Irradiation

Masahiro Tsukamoto<sup>\*</sup>, Daisuke Tone<sup>\*\*</sup>, Toshiya Shibayanagi<sup>\*</sup>, Shinji Motokoshi<sup>\*\*\*</sup>, Masayuki Fujita<sup>\*\*\*</sup> and Nobuyuki Abe<sup>\*</sup>

<sup>\*</sup>Joining and Welding Research Institute, Osaka University, 11-1 Mihogaoka, Ibaraki, Osaka 567-0047, Japan

E-mail: [tukamoto@jwri.osaka-u.ac.jp](mailto:tukamoto@jwri.osaka-u.ac.jp)

<sup>\*\*</sup>Graduate School of Engineering, Osaka University, 1-1 Yamadaoka, Suita, Osaka 565-0871, Japan

<sup>\*\*\*</sup>Institute for Laser Technology, 2-6 Yamadaoka, Suita, Osaka 565-0871, Japan

Visualization method of metal grain boundaries was developed with a short pulse laser. This visualization method was required for selecting grain in local heating system with a continuous wave (CW) fiber laser for controlling grain structures. Two kinds of short pulse lasers, nanosecond and femtosecond lasers, were used in the experiments for promoting the visualization. The sample was a stainless steel (Type 304) plate. The topography of the grain boundary regions was changed by the nanosecond laser irradiation. This topography change enabled the visualization of the grain boundaries.

DOI:10.2961/jlmn.2012.01.0025

**Keywords:** nanosecond laser, grain boundary, visualization, microstructure, crystal orientation

## 1. Introduction

Conventional heat treatments utilizing homogeneous temperature fields in electric furnaces have been commonly performed in industry to change parameters, such as type of phase, shape and size of grains, grain orientation and grain boundary structure in all material areas. Local distributions of microstructure parameters may disappear or become passive and disabled to contribute to the evolution of microstructure such as texture development. For example, during the course of cubic texture development, some cube-oriented grains cannot grow if they are surrounded by preferentially growing grains with other orientations.

In our previous study, a fiber-laser local heating system was developed in order to modify the microstructure of pure aluminum by controlling recrystallization, grain growth process and texture development[1-3]. The local heating resulted in preferential recrystallization and growth in a very small region less than 100  $\mu\text{m}$  in diameter. Orientation of the recrystallized grain can be controlled by selecting the target area precisely as well as the heating condition. The local heating resulted in grain growth even during the post homogeneous heating of the large grains formed by the spot heating. With the help from computer simulation of grain growth process for this kind of heterogeneous microstructure, a fiber laser local heating method would offer a novel technique for designing microstructures having quite different textures that had not been formed by conventional production processes. Some of the results have already been reported[1-3]. However, this laser local heating system has no function for selecting grain.

In this study, a method to visualize the grain shape with a short pulse laser was proposed. The melting point of

grain boundaries of metal is usually lower than that of the grains[4]. It was suggested that laser absorption rate at the grain boundaries was higher than that at the grains[5]. During short pulse laser irradiation, the grain boundaries visualization might be caused by slight change of the surface topography due to the melting or etching of the grain boundaries.

When a short pulse laser is available for the change of the surface topography of the metal to observe the grain's shape, the short pulse laser irradiation units will be installed in the laser local heating system. The process concept of the laser local heating system with the grain boundaries visualization unit is shown in **Fig. 1**. Microstructures such as grain shape and crystal orientation of the grains were observed with Electron Back-Scatter Diffraction pattern (EBSD[6]) equipment as shown in Fig. 1(a). After EBSD analysis, the specimen was fixed on the stage to be irradiated with the short pulse laser as shown in Fig. 1(b). The grain's shape might be visualized under suitable conditions of the short pulse laser irradiation as described above. By the comparison of the image of the surface after the short pulse laser irradiation with the EBSD image, the position of a grain with crystal orientation we would like to grow was found. The specimen can be heated by a continuous wave (CW) fiber laser irradiation immediately after the short pulse laser irradiation as shown in Fig. 1(c). Chemical and thermal etching methods for observation of grains are also good methods. However, it takes much more time for them than that for the short pulsed laser irradiation. The area modified by the femtosecond laser irradiation was compared with that done by the nanosecond laser irradiation in the experiments of the short pulse laser irradiation on the surface of stainless

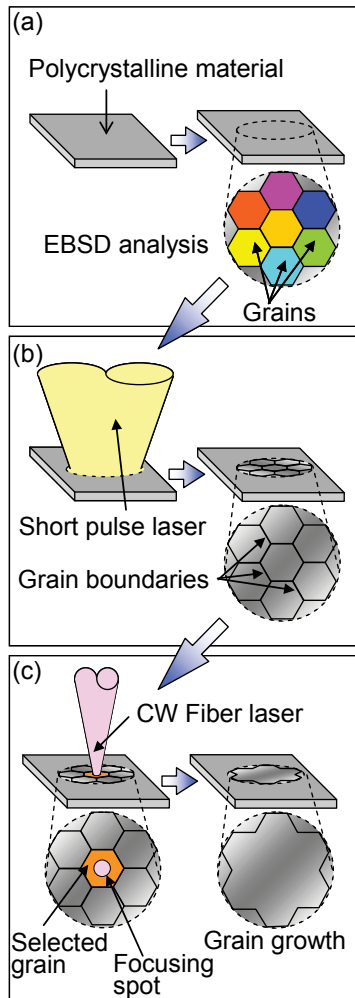


**Fig.1** (a) EBSD analysis, (b) the grain boundaries visualization with short pulse laser and (c) CW fiber laser local heating for selected grain growth.

steel. After the visualization of grain boundaries, the fiber laser was focused on the selected grain.

## 2. Experimental procedure

Schematic diagram of the experimental setup for visualizing grain boundaries with the short pulse laser is shown in **Fig. 2**. Specimens, commercial stainless steel (Type 304) plates of 1 mm in thickness, were prepared for the short pulse laser irradiation experiments as shown in **Fig. 2**. They were machined to square shape of 19 x 19 mm, with a final surface treatment by chemical polishing carried out prior to the short pulse laser irradiation. Two types of short pulse laser were used in these experiments, which were femtosecond and nanosecond lasers. The wavelength, pulse width and repetition rates of the femtosecond laser were 775 nm, 150 fs and 1kHz, respectively. For nanosecond laser, they were 1064 nm, 6 ns and 10 Hz, respectively. The specimens were irradiated with the femtosecond laser in the 100 to 500 mJ/cm<sup>2</sup> ( $6.7 \times 10^{11}$  to  $3.3 \times 10^{12}$  W/cm<sup>2</sup>) and with the nanosecond laser in the 200 to 800 mJ/cm<sup>2</sup> ( $3.3 \times 10^7$  to  $1.3 \times 10^8$  W/cm<sup>2</sup>) ranges. The laser power was controlled with an energy attenuator shown in **Fig. 2**. The numbers of pulses for the

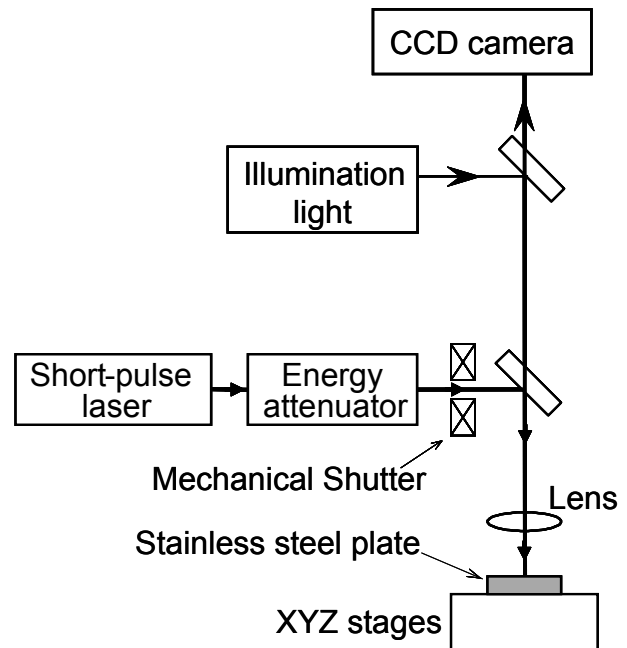


**Fig.2** Schematic diagram of experimental setup for visualizing grain boundaries with short pulse laser.

femtosecond laser and the nanosecond lasers were in the range of 10 to 50 and 50 to 300, respectively. Each laser was focused on the specimen by a lens with focal length of 150 mm. Laser beam profile of each laser on the specimen was Gaussian. Laser focusing spot diameters of femtosecond and nanosecond lasers were 60 and 170  $\mu\text{m}$  at  $1/e^2$  in intensity, respectively. Microstructure of the stainless steel plate was evaluated with an optical microscope, a scanning electron microscope (SEM), an atomic force microscope (AFM) and EBSD equipment before and after the laser irradiations.

A commercial Yb (ytterbium) fiber laser system (YLR-100-SM) for local heating of grains was employed in our system after the short pulse laser irradiation. This system provides CW laser beam at a wavelength of 1076 nm and a maximum laser power of 100 W. Diameter of the laser beam was about 7 mm after the collimator lens. The laser beam was focused on the stainless steel plate surface by a lens with a focal length of 30 mm. The stainless steel plate's position was controlled with an XYZ stage connected to a computer. A specimen, where the grain boundaries were visualized by the short pulse laser irradiation, was illuminated with the fiber laser.

## 3. Results and discussion

For femtosecond laser irradiation in the 100 to 500 mJ/cm<sup>2</sup> ranges, grain boundaries were not observed in optical image measurements. As the SEM images show, topography of the grain boundaries was not varied on the specimen although periodic nanostructures with periods of about 600 nm were produced.

For nanosecond laser irradiation, at 400 and 600 mJ/cm<sup>2</sup>, the surface morphology of the specimen was changed for over 100 pulses in optical image measurements. These changes suggest that grain boundaries were visualized with variation of topography of the grain boundaries. Optical images of the specimen surface before and after the nanosecond laser irradiation at 400 mJ/cm<sup>2</sup> for

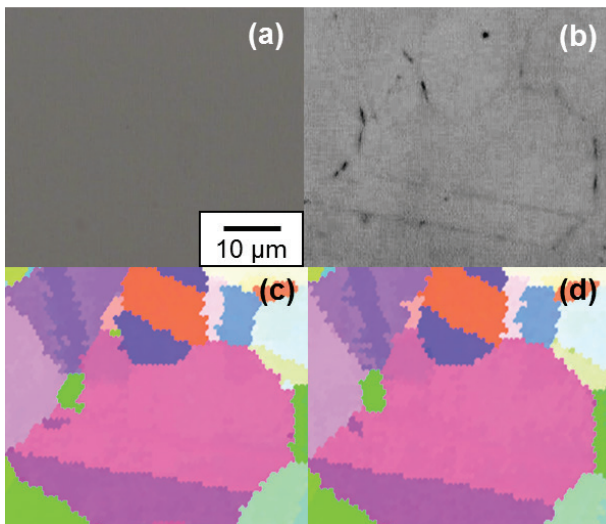


**Fig.3** Optical images of the specimen surface before and after the nanosecond laser irradiation are shown for (a) 0 and (b) 150 pulses at  $400 \text{ mJ/cm}^2$ . The EBSD patterns of the specimen surface shown in Figs. 3(a) and (b) are shown in Figs. 3(c) and (d).

150 pulses were shown in **Figs. 3 (a) and (b)**, respectively. The EBSD patterns of the specimen surface shown in Figs. 3(a) and (b) are shown in Figs. 3(c) and (d), respectively. As Figs. 3 (c) and (d) show, the grains' size and shape were not altered by the nanosecond laser irradiation. These results indicate that grain boundaries of the specimen could be visualized with nanosecond laser.

In the AFM image of the surface of the specimen shown in Fig. 3 (b), at  $400 \text{ mJ/cm}^2$  for 150 pulses, heavings were observed at the grain boundaries. For 200 pulses at  $400 \text{ mJ/cm}^2$ , heaving and caving were observed in AFM measurements. **Figure 4 (a)** shows AFM image of the specimen surface after the nanosecond laser irradiation at  $400 \text{ mJ/cm}^2$  for 200 pulses. Cross sections at (a1) and (a2) in Fig. 4 (a) are shown in Figs. 4 (b) and (c), respectively. The results of this analysis indicate that heaving and caving of grain boundaries. The height of the heaving and the depth of the caving regions were  $47 \text{ nm}$  and  $76 \text{ nm}$ , respectively, as shown in Figs. 4 (b) and (c). For over 200 pulses, the crystal orientations in the vicinity of the grain boundaries, where they have the caving as shown in Fig. 4 (c), were not observed in the EBSD analysis. For 300 pulses, periodic microstructures[7] were partially formed on the specimen surface. It was also difficult to measure the crystal orientations of grains with the periodic microstructures.

As Figs. 3 (c) and (d) show, grain growth was not caused by the nanosecond laser irradiation. When grain boundaries were visualized as shown in Fig. 3 (b), laser intensity of the nanosecond laser on the specimen was  $6.6 \times 10^7 \text{ W/cm}^2$  for laser fluence of  $400 \text{ mJ/cm}^2$ , which was close to the ablation threshold[8]. Then, temperature of the grains' surface could be increased to a temperature near the melting point of the grain during the nanosecond irradiation. However, pulse duration of the nanosecond laser was  $6 \text{ ns}$ . In our previous study, the specimen was irradiated with CW fiber laser at the output power of  $10 - 100 \text{ W}$  for over  $10 \text{ s}$  to cause the grain growth. Thus, heating time with

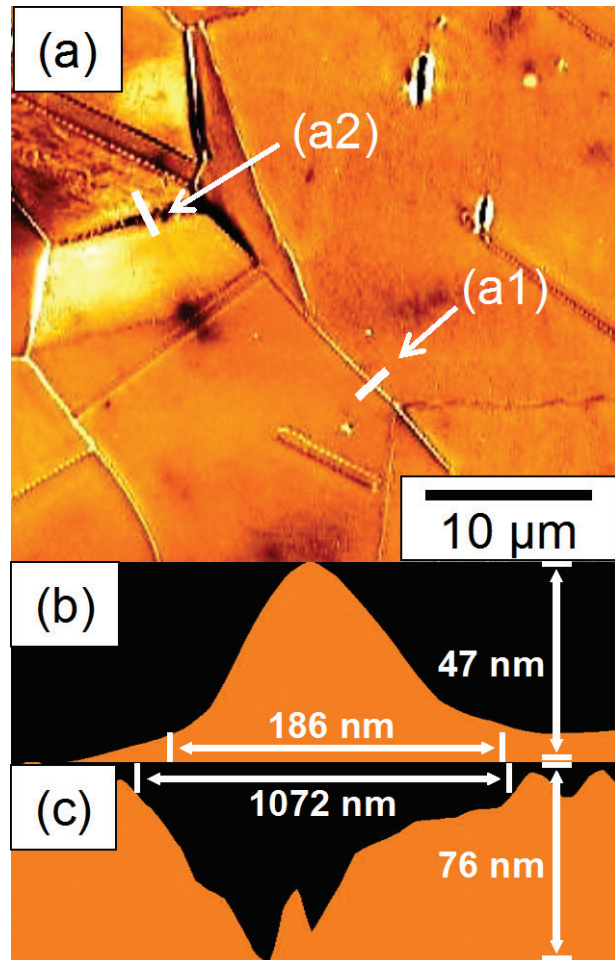


**Fig.4 (a)** AFM image of specimen surface after the nanosecond laser irradiation at  $400 \text{ mJ/cm}^2$  for 200 pulses. Cross sections at (a1) and (a2) in (a) are shown in (b) and (c), respectively.

nanosecond laser might be too short to cause the grain growth. In the typical experimental condition for the grain growth, irradiation time, output power and spot diameter on the specimen of CW fiber laser were  $15 \text{ s}$ ,  $10 \text{ W}$  and  $10 \mu\text{m}$ , respectively. Then, fluence was  $2 \times 10^8 \text{ J/cm}^2$ . For the nanosecond laser irradiation to visualize grain boundaries as shown in Fig. 3 (b), fluence for  $15 \text{ s}$  was  $60 \text{ J/cm}^2$  since fluence per pulse, number of pulses for the visualization and the repetition rate were  $400 \text{ mJ/cm}^2$ ,  $150$  and  $10 \text{ Hz}$ , respectively. Thus, fluence for the visualization with nanosecond laser was much smaller than that for the grain growth with CW fiber laser. Thus, fluence for  $15 \text{ s}$  with the nanosecond laser might be too small to cause the grain growth.

Thermal etching process is also heating process to visualize the grain boundaries. However, the process with nanosecond laser we proposed in this study is different from the thermal etching process. The differences between the both processes are mechanisms to change the topography of the grain boundaries. The topography of grain boundaries' surface is changed from flat to concave in the thermal etching process. In the process with nanosecond laser, the topography of the grain boundaries' surface was changed from flat to the convex at first stage as

shown in Fig. 4(b). These results indicate that mechanism of the topography variation of the grain boundaries surface by the nanosecond laser irradiation was different from that by the thermal etching. In the process with nanosecond laser, the surface of the specimen was heated for 6 ns, the time of pulse duration. Heating time in the process with nanosecond laser was much shorter than that in the thermal etching. Interval time between the pulses was 100 ms since the repetition rate of the nanosecond laser was 10 Hz. After one pulse, the surface was cooled down in 100 ms. The surface was heated for 6 ns again by next pulse irradiation. Thus, it is interpreted that height of the heaving at the grain boundaries was increased as number of pulses was increased until 150 pulses. This interpretation suggests that mechanism of the topography variation of the grain boundaries surface by the nanosecond laser irradiation was different from that by the thermal etching

As described before, laser intensity,  $6.6 \times 10^7 \text{ W/cm}^2$  for  $400 \text{ mJ/cm}^2$ , was less than ablation threshold [8]. If heaving of the grain boundaries is caused due to nanosecond laser ablation, ablation rate of grains should be bigger than that of grain boundaries. Then, absorption rate of laser light on grain surface must be larger than that of grain boundaries or melting point of grain must be lower than that of grain boundaries. However, as indicated in Refs. 4 and 5, absorption rate of laser light on grain surface is smaller than that on grain boundaries and melting point of grain is higher than that of grain boundaries. Thus, heaving of the grain boundaries could not be caused due to nanosecond laser ablation.

Heaving and caving of the grain boundary regions might be caused due to the difference of the melting point between the grain and the grain boundaries. Since the melting point of the grain boundaries is usually lower than that of the grain [4], the grains are not melted when the grain boundaries are melted. The grains are slightly expanded with heat given by the laser irradiation. Melted grain boundary regions are pushed by the expanding grains. Thus, shape of the grain boundary region is changed from flat to convex. During or after the pushing, grain boundary region is solidified by natural cooling. Then, heaving of the grain boundary region was produced. Laser absorption rate of heaving region is higher than that of flat region. Therefore, the heaving region is ablated selectively during the laser irradiation. By the ablation of the heaving region, caving of the grain boundary region might be formed. In the future, additional measurements in the experiment with a nanosecond laser will be performed with intent to report a more detailed analysis of the topography changes of grain boundaries.

In this experiment, the grain boundaries could be visualized. However, since shape of the nanosecond laser beam profile on the specimen was Gaussian as described above, good visualization of the grain boundaries was obtained in the center area of the laser irradiation area. When shape of the laser beam profile is the flat top type, good visualization of the grain boundaries can be obtained in whole area of the laser irradiation. Maximum output energy per pulse of our nanosecond laser is 900 mJ. In this experiment, fluence required for the visualization of the grain boundaries was  $400 \text{ mJ/cm}^2$ . Therefore, grain

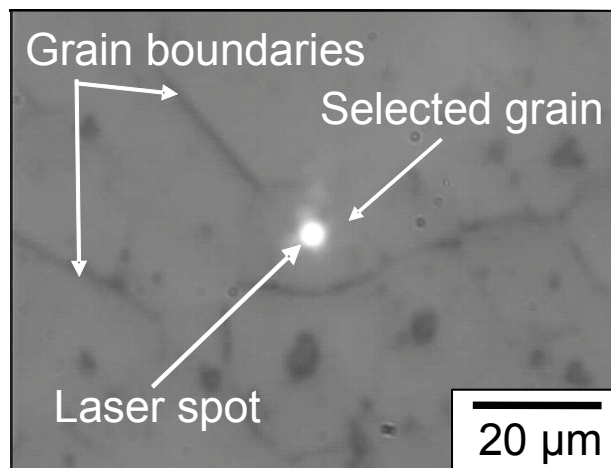


**Fig.5** The optical image of the specimen surface monitored with CCD camera. The selected grain could be illuminated with a CW fiber laser.

boundaries in the area of  $2.2 \text{ cm}^2$  will be able to be visualized by using our nanosecond laser.

The optical image of the specimen surface monitored with CCD camera was shown in **Fig. 5**. Figure 5 indicates that the selected grain could be illuminated with a CW fiber laser.

#### 4. Summary

The observation system of grain boundaries on the stainless steel plate surface with a short pulse laser was proposed. The area created by femtosecond laser irradiation was compared with that by nanosecond laser irradiation in the experiments of laser irradiation to the surface of stainless steel. After femtosecond laser irradiation, a grain boundary was not observed, however, after nanosecond laser irradiation, a grain boundary was observed. The EBSD pattern of the stainless steel after nanosecond laser irradiation was similar to that before the irradiation. This indicates that the grain size and shape were not changed by nanosecond laser irradiation. Thus, a grain boundary visualization system could be obtained by the method with the nanosecond laser. AFM analysis indicates that heaving and caving were caused at the grain boundaries by nanosecond laser irradiation.

#### References

- [1] M. Tsukamoto, T. Shibayanagi, H. Nakano, T. Yamashita, Y. Soga and N. Abe: ICALEO 2007 Congress Proceedings, (2007) p.75. (Journals)
- [2] T. Shibayanagi, M. Tsukamoto, T. Matsumoto, Y. Soga, and N. Abe: Materials Science Forum, 558-559, (2007) p.329. (Journals)
- [3] T. Shibayanagi, M. Tsukamoto, N. Matsuda, Y. Soga, N. Abe and M. Naka: Solid State Phenomena, 127, (2007) p. 337. (Journals).
- [4] K. Kobayashi, K. Ikeuchi, K. Nishimoto: Zairyousetugoukougakunokiso, (2000) p.125
- [5] J. Yan, T. Asami, and T. Kuriyagawa: Semiconductor Science and Technology, 22, (2007) p. 392. (Journals).
- [6] T. Shibayanagi: Journal of High Temperature Society, 29, 4, (2003) p.123. (Journals)
- [7] M. Tsukamoto, K. Asuka, H. Nakano, M. Hashida, M. Katto, N. Abe, and M. Fujita: Vacuum. 80, (2006) p.1346. (Journals).
- [8] M. Fujita: Kougaku, 36, 8, (2007) p.459. (Journals).

(Received: March 28, 2011, Accepted: December 19, 2011)